2017 International Symposium on Nonlinear Theory and Its Applications,
NOLTA2017, Cancun, Mexico, December 4-7, 2017

Broad Spectrum Nonlinear Channelizer

Antonio Palacios†, Visarath In‡ and Patrick Longhini‡

†Nonlinear Dynamical Systems Group, Department of Mathematics,
San Diego State University, San Diego, CA 92182, USA
‡Space and Naval Warfare Systems Center, Code 71730
53560 Hull Street, San Diego, CA 92152-5001, USA
Email: apalacios@mail.sdsu, visarath@spawar.navy.mil, patrick.longhini@navy.mil

Abstract—The Nonlinear Channelizer is an integrated circuit made up of large parallel arrays of analog nonlinear oscillators coupled unidirectionally. Collectively, the arrays serve as a broad-spectrum analyzer with the ability to receive complex signals containing multiple frequencies and instantaneously lock-on or respond to any arbitrary input Radio Frequency (RF) signal in a few oscillation cycles. This manuscript provides a review of the theory, numerical simulations and some engineering details that validate the concept, modeling, design and fabrication.

1. Introduction

The Nonlinear Channelizer circumvents the traditional approach to RF signal detection and locking by exploiting the nonlinear input-output characteristics of nonlinear oscillators and collective behavior achieved by certain coupling topologies. In particular, the system employs synchronization [1, 2] similar to that of coupled Van der Pol system [3, 4], but it is constructed of three or more one-dimensional *overdamped* bi-stable elements. These overdamped elements cannot oscillate in the absence of coupling, as oppose to Van der Pol oscilaltors which can oscillate endogeneously, i.e., on their own. However, the coupling-induced oscillations can lead to significant savings in cost and power requirements.

In a nutshell, a "Nonlinear Channelizer" can be described simply as a RF spectrum analyzer contained on an analog microchip, which can perform its function on a massively parallel scale, as denoted in the Channelizer IC in Fig. 1 and Fig. 4. Each chip is capable of having hundreds of discrete arrays of coupled nonlinear oscillators, with each array adjusted to cover a specific frequency range for signal interception. Figure 4 shows how the channels can be stacked over a wide range of frequencies to cover the spectrum of interest. In operation, the entire incoming frequency spectrum gathered by an antenna or the system front-end is fed to all the banks (channels) of oscillators for channelizing. If the incoming signal has frequency content which falls within the range (within the V-shape or bandwidth) of a specific bank (channel), then the oscillators in that bank would change their natural oscillation's characteristics to lock-on to that signal in response; even though the incoming signal may be off from the natural oscillation's frequency. While responding to the input signal, each oscillator in the channel array oscillates at f_{in}/N, where f_{in} is the input signal frequency and N is the number of nonlinear oscillators coupled in the array (N is odd and greater than 1). This effect provides an automatic frequency down-conversion function to bring the intercepted signal from high to low without using the commonly employed method of frequency mixing in state-of-the-art communication systems. The lowering of the frequency makes it easy for signal digitization via a commonly available Analog-to-Digital system. Afterward the responding channels outputs can be passed on to the Control and Logic electronics for further signal processing, which are denoted as the back-end in Fig. 1.

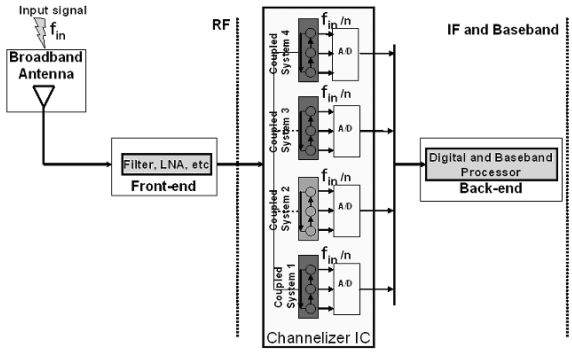

Figure 1: Schematic concept of a Nonlinear Channelizer. The device is essentially a RF spectrum analyzer made up of hundreds of discrete arrays of coupled nonlinear oscillators. Each array is tuned to cover a specific frequency range for signal interception.

2. Modeling and Analysis

The basic dynamics of the N-element array can be modeled, see [5, 6], through the following system of differential equations,

$$C_L \dot{V}_i = -gV_i + I_s \tanh(cV_i) - I_c \tanh(cV_{i+1}) + I_g \tanh(cs(t)), \quad (1)$$

where $i = 1, \ldots, N$. Note that we have cyclic boundary conditions, the array is actually an N-element "ring" with unidirectional or forward coupling only. C_L is the effective load capacitance of the entire circuit, which sets the

maximum response time of the circuit. I_s is nonlinear coefficient that the defines the bistability of the circuit when tuned passed a threshold value. I_c is the coupling coefficient between the nonlinear oscillators. I_g controls the input gain from an external time varying signal $s(t)$, and c is a constant based on the microchip process. Typical parameter values are: $C_L = 0.1pF$, $g = 1/1000\Omega$, $c = 7$, $I_s = 900\mu A$, $I_c = 650\mu A$, $I_g = 100\mu A$.

2.1. Bifurcation Diagram

We now consider $s(t) = \varepsilon \sin(2\pi\omega t)$, where ε represents the amplitude of the incoming signal (sinusoidal) and ω is the frequency. In the absence of the external signal ($\varepsilon = 0$), the system is known to exhibit quiescent steady-state behavior as well as oscillatory behavior. In the oscillatory state, each component switches between its two stable states, leading or lagging its neighboring component by $2\pi/N$ radians. Again, this pattern is referred to as the out-of-phase or traveling wave pattern [5, 6, 7]. Figure 2 illustrates three regions of response to a signal as a function of amplitude ε and the parameter I_c representing the strength of the coupling between the components of the ring.

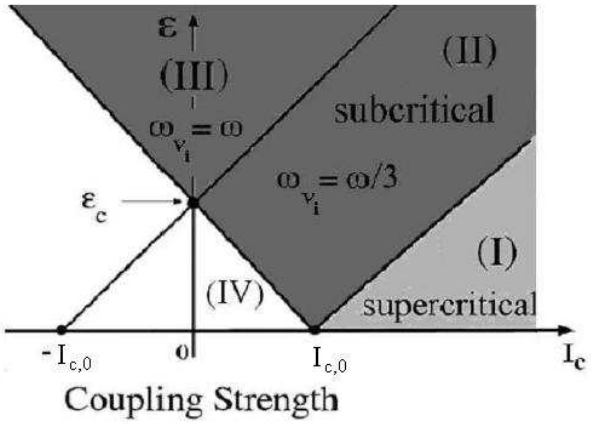

Figure 2: Bifurcation diagram depicting different regions of behavior in a channelizer, with three elements per array, as a function of inter-component coupling strength I_c and signal strength ε. Regions (II) and (III) represent synchronization with an external signal with frequency ω. In region (II) each oscillator oscillates at $\omega/3$. In region (IV) the system does not oscillate. In Region (I) the oscillators in the array do not lock onto the incoming signal. Instead, they oscillate at their natural frequencies.

In the supercritical region (I) the oscillator is not frequency locked to the incoming signal, rather it oscillates at its natural frequency. In region (II) the oscillator is frequency locked to the incoming signal so that each component of the oscillator switches at a frequency that is ω/N, where ω is the frequency of the incoming signal and N is the number of components in the oscillator. In region (III) the dynamics of each component is over-driven by the incoming signal, resulting in an in-phase response with respect to each other and the signal. The significance of regions (II) and (III) is that in those regions the response of the oscillator is overwhelmingly driven by the characteristics of the incoming signal $s(t)$ in terms of phase and frequency. In this sense the oscillator channels the significant qualities of the incoming signal. Even in the case of frequency down-conversion, which occurs in region (II), the phase information of the input signal is preserved via the synchronization effect. Thus, a theoretical and experimental understanding of parametric control over the regions of synchronization and the bifurcation qualities will be necessary to design channelizing devices that accurately target signals with precise frequency and amplitude characteristics.

2.2. Frequency Response

Consider now the case where the system is operating in region I, so that the channelizer is in the oscillatory state. The black curve in Figure 3 shows a frequency response of 267.03MHz when $\varepsilon = 0$. Upon applying a dc signal, with $\varepsilon = 0.5$, the frequency shifts to 219.35MHz, as is shown by the green curve. When an ac signal is applied, instead of just dc, there is an additional effect in which the channelizer downconverts the frequency of the incoming ac signal by a factor of N, in the example of Figure 2 the downconvertion factor is $N = 3$. Thus applying a 1.0GHz sinusoidal signal to the channelizer generates an output where each element oscillates at 0.333GHz, see the red curve in Figure 3.

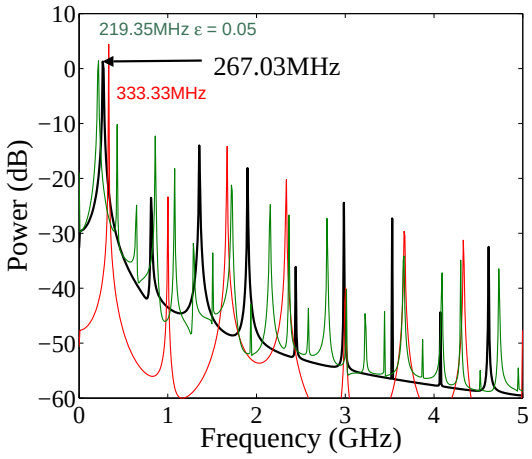

Figure 3: (Color online) Typical Frequency Response of a Nonlinear Channelizer. The green curve is the response of the channelizer to a dc input signal with $\varepsilon = 0.05$. Red curve is the response to an ac input signal oscillalting at 1GHz.

2.3. Locking into Synchronization

Figure 4 illustrates through numerical simulations the effect of tuning the coupling parameter I_c to create a *stacking effect*, i.e., building the channelizer to cover a wide spectrum of interest. Other parameters may be tuned in a similar fashion, to customize the shape of the channel (V-shape). The width of the V-shape is associated to the

bandwidth of the channel for a given signal amplitude ε. The parameter space sweeps the input signal amplitude vs. input signal frequency for three different channels denoted by $I_c = 650\mu A$, $I_c = 750\mu A$, and $I_c = 850\mu A$. It is, effectively, showing the ability to configure the system to act as channels according to the various V-shape regions. In the configuration of the channelizer, the V shapes are stacked one next to the other to be able to process the different frequencies across a wide spectrum contained in the input signal, as is illustrated in Fig. 4. Each V shape is a channel capable of taking a band of frequencies as determined by a designer. Their widths can be tuned by adjusting the parameters of the circuits to either widen or narrowing the channel effect.

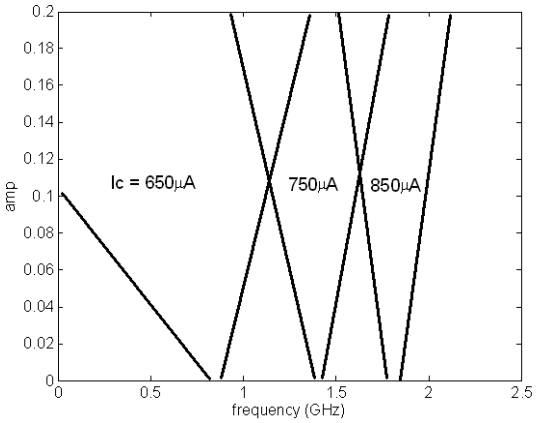

Figure 4: Arnold's tongue showing the V shaped region of synchronization defined by the amplitude of the input signal ε and the difference between the signals frequency ω and the natural frequency ω_N.

By setting up the channelizer to operate in region I of Fig. 2 (prior to receiving an input signal), the dynamics of the channelizer can transition to region (II) by changing ε from a small to a larger amplitude. Figure **??** depicts the transition with the minimal amplitude to lock-on via the frequency spectrum. It is clear from Fig. **??** that the onset of locking onto a single tone occurs when all other frequency mixing vanishes near the top of the graph. Assuming the amplitude to be greater than the critical amplitude for lock on, Fig. 5 demonstrates that by varying the input frequency the channelizer can unlock once the input frequency crosses the boundary (bandwidth) of that V-shape. The black dashed line in Fig. 5 represents $1/3$ the frequency of the applied "target" signal. The channelizer follows the input frequency, however, when the frequency becomes out of band or channel it unlocks.

3. Hardware Implementation

In this section we implement the schematic concept of a Nonlinear Channelizer for the particular case of three coupled nonlinear elements. We stress that the extension of the

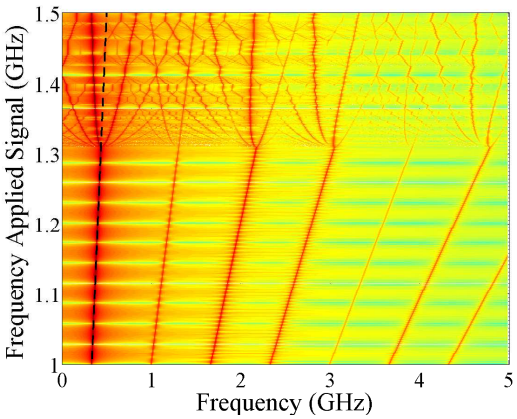

Figure 5: (Color online) Frequency locking/unlocking in a Nonlinear Channelizer by simply varying the frequency of the input signal.

implementation to N elements in the array is quite straightforward and follows, naturally, from our current results.

3.1. Design of Single Overdamped Element

Each element in the array is described by an overdamped bistable system containing the hyperbolic tangent function as the nonlinear term, which results from using an Operational Transconductance Amplifier (OTA) to perform this function. To construct a channel, each element has to have the ability to receive a signal and output a signal to provide the information to the adjacent element in the array configuration. The coupling function is performed by another OTA. Additionally, the element also has to have the ability to take in the drive (target) signal for detection, which is also performed by another OTA. In total, each nonlinear element in the array contains three OTA's: the first one provides the nonlinearity in the dynamics, the second one executes the coupling function, and the third one produces the input for the drive signal. Figure 6 illustrates in more detail the layout of the nonlinear element with these functionalities being implemented with various parts labeled according to their interconnections.

The dynamics of the coupled system can be derived from the circuit analysis and is suitably described by

$$C_L \dot{V}_i = -gV_i + I_s \tanh(c_s V_i) - I_c \tanh(c_c V_{i+1}) + I_g \tanh(c_g s(t)), \quad (2)$$

where I_c and c_c control the coupling strength inside the array, the I_g and c_g control the gains of input signal, and $s(t)$ is the input signal, mainly a sinusoidal or an FM modulated signal for the experiment. The variable V_i represents the voltage output of the i^{th} element in a uni-directionally coupled N-element ring oscillator, where $i = 0, 1, \ldots, N-1$. The parameters c_s, c_c, c_g are the inherent capacitances of the operational transconductance amplifiers used to build the nonlinear part of the circuit. They are not changeable once the circuit is designed and fabricated. In our circuit, these capacitances take the values $c_s = c_c = c_g = \frac{1}{7V}$.

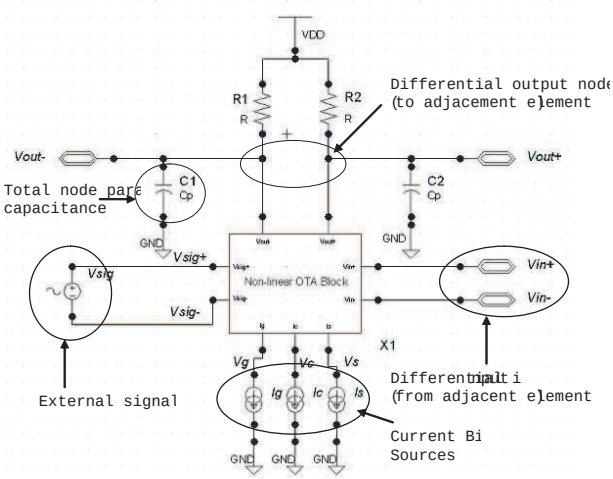

Figure 6: Detail layout of a single element of the Nonlinear Channelizer in the microcircuit.

Once the circuit of a single element is defined, the entire array can be constructed by connecting three elements together to form a channel. The differential outputs of each element are connected to the on-chip buffers made up of a single emitter-follower stage to prevent the load from affecting the oscillator's behavior and to provide the necessary system isolation when the signals are extracted from each element in the array. Figure 7 shows the chip layout which contains four channels on a 2mm x 2mm footprint.

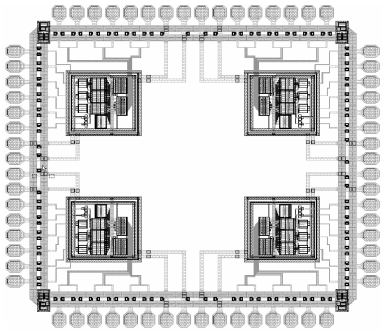

Figure 7: Circuit Layout with four channels are placed within the same chip. A single pad is used for each input and output.

After the microchip is fabricated, it is integrated onto a test board (not shown for brevity), where it has all of the necessary support components to provide power, biasing currents and tuning elements, to bring the entire system into operation.

Figure 8 demonstrates that increasing I_c results in increasing the oscillation frequency which shifts the center of the V shape to the right. For example, setting $I_c = 407\mu A$ the center is around 900 MHz. Then adjusting I_c to $542\mu A$ the center shifts to 1.20 GHz and so on in shifting to 1.50 GHz and 1.80 GHz as indicated in the figure. Notice that the width of the channel decreases as the system moves to higher frequencies, which was also observed in numerical simulations shown in Fig. 4. To configure the bandwidth of the channel, I_g may be tuned to widen or narrow the channel via a similar control of the feedback current.

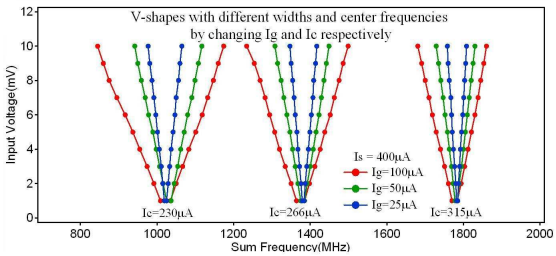

Figure 8: (Color online) Experimental results of V-shape displacements, through changes in coupling strength I_c, create the stacking effect to build a channelizer.

4. Conclusions

We have review the capabilities of an integrated circuit, named the *nonlinear channelizer*, to receive complex signals of multiple frequencies and instantaneously lock-on or respond to an arbitrary input Radio Frequency (RF) signal. These capabilities are achieved by exploiting the collective behavior of arrays of nonlinear oscillators coupled in a specific fashion. Throughout the manuscript we reviewed the fundamental theory and bifurcation analysis that helped design the nonlinear channelizer.

Acknowledgments

We wish to acknowledge support from SPAWAR Systems Center Pacific's S&T Program (internal funding), US Airforce, and the Office of Naval Research (Code 30). A.P. were supported in part by National Science Foundation grants CMMI-0638814 and CMMI-0625427.

References

[1] A. Balanov, N. Janson, D. Postnov, and O. Sosnovtseva. *Synchronization: From Simple to Complex*. Springer, (2009).

[2] A. Pikovsky, M. Rosenblum and J. Kurths. *Synchronization*. Cambridge, (2001).

[3] B. van der Pol. *Phil. Mag.*, 3:64–80, 1927.

[4] B. van der Pol. *Nature*, 120(3019):363–364, 1927.

[5] V. In, A. Kho, J. Neff, A. Palacios, P. Longhini, and B. Meadows. *Physical Review Letters*, 91(24):244101–244101–4., (2003).

[6] V. In, P. Longhini, A. Kho, N. Liu, S. Naik, A. Palacios, and J. D. Neff. *Physica D*, 240:701–708, April 2011.

[7] P. Longhini, A. Palacios, V. In, J. D. Neff, A. Kho, and A. Bulsara. *PRE*, 76(2):026201, August 2007.